Separation and Purification Technology 289 (2022) 120727

Contents lists available at ScienceDirect

Separation and Purification Technology

journal homepage: www.elsevier.com/locate/seppur

Wire-wrapped and helically-finned tubular ceramic membranes for enhancing water and waste heat recovery from wet flue gas

Chao Ji, Wei Liu, Hong Qi *

College of Chemical Engineering, Nanjing Tech University, Nanjing 210009, China

ARTICLE INFO

Keywords:
Flue gas dehumidification
Water recovery
Transport membrane condenser
Fin tube
Wire-wrapped tube

ABSTRACT

Recycling water and waste heat from wet flue gas is crucial for sustainable energy-water-environment nexus in industrial processes. Herein, we report the use of wire-wrapped and helically-finned tubular ceramic membranes to construct membrane condensers for simultaneous water and heat recovery. Compared with conventional plain tubular ceramic membrane (PTCM), wire-wrapped tubular ceramic membrane (WTCM) and helically-finned tubular ceramic membrane (FTCM) both exhibit superior water and heat recovery performance, indicating a non-negligible effect of chaotic fluid mixing on heat and mass transfer enhancement. FTCM shows better condensate capture performance than WTCM. Moreover, improved condensing heat transfer performances are observed on FTCMs provided with large fin height and pitch. FTCM provides higher heat transfer coefficients than PTCM at around 7.4% to 59.3% depending on different fin structures. Effects of operation parameters on membrane condensation process using FTCM are also investigated. Gas-side parameters have significant effects on water/heat recovery performance than water-side parameters. This study can serve as a basis for process intensification of membrane-based condensation used for flue gas dehumidification.

1. Introduction

Sustainable energy-water-environment nexus has come into focus in power generation industry in recent years. Thermal power plants have become the largest water consumer while providing energy guarantee for rapid social and economic development. 41% of available water in the United States is used for power generation.[1] Apart from high thirst for freshwater, massive emission of high-humidity flue gas is another challenge for thermal power plants. The flue gas, exhausted under near-saturated conditions, contains large amount of water and latent heat resources. For a typical 600 MW lignite genset, the amount of water vapor discharged with flue gas is approximately 2.6×10^5 $Nm^3 \cdot h^{-1}$.[2] Through recovering 20% of vapor from the exhaust, thermal power plants can realize near-zero consumption of water.[3] The reasonable use of low-grade waste heat recovered along with water vapor can effectively enhance the energy efficiency of power plants. Moreover, emission of wet flue gas may lead to chimney corrosion, white smoke plume, and other environmental issues.[4] Wet flue gas impedes the diffusion of pollutants, and the resulting haze reduces visibility. The optical properties of hygroscopic aerosols change in wet environment, leading to the colored smoke plume.[2] Recycling water from high-humidity flue gas can not only alleviate environment problems around power plants, but also improve the water-saving ability and thermal energy efficiency. Therefore, efficient flue gas dehumidification and water recovery technology is of great significance for sustainable energy-water-environment nexus.

Typical approaches of the flue gas dehumidification and water recycling principally include liquid absorption,[5] condensing heat exchange,[6] and membrane technology.[7] Water vapor can be easily removed from flue gas using absorbents such as calcium chloride ($CaCl_2$), lithium chloride (LiCl), potassium formate (KCOOH) in absorption tower.[8] However, challenges remain for the liquid absorption method, that is, the huge energy consumption for absorbent regeneration on the one hand, and the treatment of deposits formed by the contact of flue gas with absorbent on the other hand.[4] Heat exchangers made of stainless steel are widely used in condensing and recycling water vapor from flue gas, but disadvantages are still presented as follows. 1. Low-temperature corrosion caused by acid gases in

Abbreviations: PTCM, plain tubular ceramic membrane; WTCM, wire-wrapped tubular ceramic membrane; FTCM, helically-finned tubular ceramic membrane; TMC, transport membrane condenser; HTEs, heat transfer enhancement techniques; CNC, computer numerical control; PVDF, poly(vinylidene fluoride); SPEEK, sulfonated poly(ether ether ketone); PES, polyethersulfone.

* Corresponding author.
E-mail address: hqi@njtech.edu.cn (H. Qi).

https://doi.org/10.1016/j.seppur.2022.120727
Received 5 December 2021; Received in revised form 22 January 2022; Accepted 20 February 2022
Available online 23 February 2022

flue gas reduces the equipment lifespan. Thus, corrosion-resistant coatings [9] and fluorine plastic tubes [10] are developed. 2. A fouling layer consisting of fly ash and condensate can easily form and therefore reduce the heat exchanger efficiency by 13–22%.[11] 3. The recovered low-quality water needs further treatment. In recent years, membrane technology has been investigated for recycling water from flue gas, for its easy operability, simple device, excellent chemical stability, non-corrosiveness, and high-quality recovered water. Membrane processes applied for flue gas dehumidification include vapor permeation and membrane condensation.[7] For vapor permeation, dense membranes are employed to selectively separate water vapor from other gases via sorption–diffusion mechanism. Sijbesma et al. first confirmed the technical viability of flue gas dehumidification using dense polymer membranes by a pilot test in a thermal power plant.[12] Vapor permeation membrane has impressive permselectivity, but its water recovery performance depends on the vacuum permeation capacity.[7] In addition, vapor condensation inside porous support (e.g., hollow fiber) should be avoided in practical application.

In membrane condensation, hydrophilic or hydrophobic porous materials are used for recovering water from the flue gas. The dehumidification mechanisms of membranes with two kinds of wettability are illustrated in Fig. 1. Macedonio et al. developed a membrane condenser based on porous hydrophobic organic membranes such as poly(vinylidene fluoride) (PVDF) membranes for wet flue gas dehumidification.[13,14] Water vapor condenses on the hydrophobic surface following the principle of dropwise condensation, whereas partial dehumidified gas permeates through the membrane, as shown in Fig. 1a. To minimize the impact of contaminants on long-term operational performance, membranes with high hydrophobicity are required for this process.[15] In addition, the thermal conductivity of polymer membranes needs to be improved to enhance the vapor condensing ability. Based on porous hydrophilic ceramic membranes, the innovative concept of transport membrane condenser (TMC) was introduced by Wang et al. from the Gas Technology Institute.[16] As illustrated in Fig. 1b, the vapor condenses on the outer surface and/or in the pores, then continuously permeates through the ceramic membrane under slightly negative pressure on the water side. Non-condensable gases cannot pass through the membrane because condensate clogs the pores. TMC can simultaneously recover latent heat and water from wet flue gas to circulating water. With high mechanical stability, remarkable thermostability, excellent acid and alkali resistance, and long lifespan, porous ceramic membranes are promising materials for water recovery in complex flue environments.

Many researchers have experimentally investigated TMC for water recovery from flue gas, and relevant literatures on parameters and performance of TMCs are summarized in Table 1. Based on the comparison of tubular porous ceramic membranes with conventional stainless steel tubes under the same characteristic size, Bao et al. found that the Nusselt numbers of tubular ceramic membranes are 50–80% higher than those of stainless steel tubes. For stainless steel tubes, condensate accumulates on the impermeable surface and condensate film inhibits the heat transfer.[17] An 800 h continuous pilot test of TMC carried out by Wang et al. achieved the water recovery efficiency of 40–55%.[16] Many follow-up works focus on the effects of different operation parameters (cooling water parameters, flue gas parameters, and transmembrane pressure difference) on flue gas condensation performance of TMC.[18–20] Further researches in terms of pore size,[21] multi-channel membrane,[22] multistage condenser,[23] tube pitch,[24] and hydrophilic/hydrophobic treatment,[25] are reported in recent years. In addition, numerical simulations, such as entropy generation model[26] and hybrid condensation model,[27] are also conducted to analyze the heat and mass transfer mechanism in TMC. The feasibility of the TMC for flue gas dehumidification, as well as the pilot-scale investigation are also performed in our group.[22–23,28–31]

According to the literatures, the major concerns on the practical industrial applications of TMC are membrane area, equipment size, investment cost, fly ash accumulation, etc. For the thermal power plant (600 MW), the emission of flue gas is approximately 2×10^6 $Nm^3 \cdot h^{-1}$.[2] Treating a gas of this size requires a large membrane area, which will cause a rise of equipment size and investment cost. In fact, we believe that the above problems can be solved by two strategies. 1. Further improving the condensing performance of TMC can reduce the membrane area, such as designing compact heat exchanger. Heat transfer enhancement techniques (HTEs) which can improve the thermal

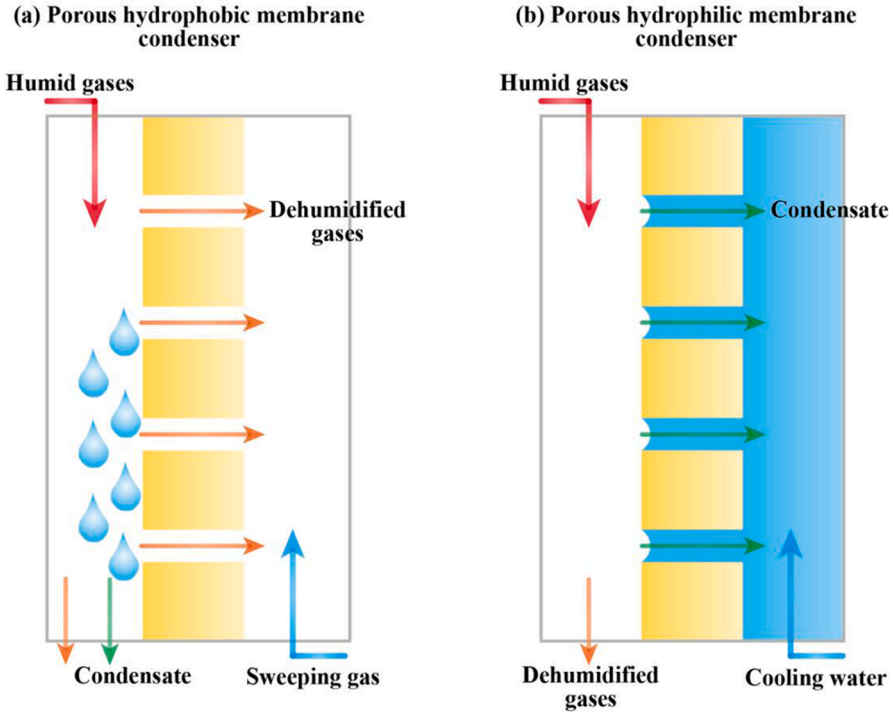

Fig. 1. Membrane condenser configurations of (a) porous hydrophobic membranes and (b) porous hydrophilic membranes.

Table 1
Performances of TMC for Flue Gas Dehumidification.

Pore size (nm)	Flue gas temperature (°C)	Maximum flue gas flowrate ($m^3 \cdot h^{-1}$)	Membrane area (m^2)	Highest water flux ($kg \cdot m^{-2} \cdot h^{-1}$)	Notes	Reference
1000	50	10,000	14.28	43.65	Pilot scale, Coal-fired boiler exhaust	Ref.[32]
1000	50	10,000	1.176	22.23	Pilot scale, Coal-fired boiler exhaust	Ref.[24]
1000	40–60	1600	0.7	15.77	Lab scale, Gas-fired boiler exhaust	Ref.[11]
20, 30, 50, 100	50–70	1.08	0.025	5.4	Lab scale, Simulated gas, vapor/N_2	Ref.[21]
40, 90	60–80	0.36	0.00716	13	Lab scale, Simulated gas, vapor/air	Ref.[33]
5, 20, 50	50–65	100	0.3	38.5	Lab scale, Simulated gas, vapor/air	Ref.[23]
20	50–70	0.48	0.0377	15	Lab scale, Simulated gas, vapor/N_2	Ref.[19]
8–10	45–85	0.78	0.1043	4.2	Lab scale, Simulated gas, vapor/air	Ref.[22]
7	80–120	0.42	0.0021	8	Lab scale, Simulated gas, vapor/air	Ref.[18]
6–8	65–95	75	0.582	6.3	Lab scale, Gas-fired boiler exhaust	Ref.[17]

property of heat exchangers are conducive to reduce the heat exchanger size and operating cost.[34] So far, relevant information is unavailable in the literatures on HTEs of porous membrane-based condensers. 2. Symmetric ceramic membranes, which have a uniform and homogenous structure along the direction of membrane thickness, can be employed to construct TMC. The costs of ceramic membranes are around 2000 USD $/m^2 according to Dilaver et al.[35] Multiple sintering of the multi-layered asymmetric structure and high-temperature firing result in high cost of ceramic membranes. According to Table 1, the water flux of TMC process lies in the range of 0–50 $kg \cdot m^{-2} \cdot h^{-1}$. Current TMC process is controlled by condensation process, not permeation process.[1] Thus, symmetric ceramic membranes can be used to construct TMC to reduce the investment cost.

The thermal resistance of TMC is mainly on flue gas side.[36] Clearly, appropriate HTEs should be introduced to promote convection-condensing heat transfer of flue gas, which is the key factor to increase performance of TMC. Passive HTEs by using various enhancers have received increasing attention as it does not need external power. From geometrical point of view, these enhancers include surface-enhanced tubes (i.e., fin tube, corrugated tube, helical tube, microfin tube, etc.), wires, and tapes.[37] Owing to strong turbulence effect and large surface area, fin tubes show higher heat transfer rates than plain tubes, and thus, installation footprint and manufacture costs for heat exchangers can be reduced.[38] Wrapping the tube with wires is a simple and cheap method in HTEs as there is no machining required.[39] Hence, a new strategy of combining various enhancers with porous ceramic membrane is introduced to improve the flue gas condensation performance in TMC process.

In the current paper, wire-wrapped and helically-finned porous ceramic membranes are first proposed to construct TMC for recycling water and waste heat from wet flue gas. With the heat transfer enhancement techniques, membrane area and TMC size are expected to be reduced in practical applications. Symmetric tubular ceramic membranes were selected, and an experimental system of TMC was built. The water and heat recovery performances of conventional plain tubular ceramic membrane, wire-wrapped tubular ceramic membrane and helically-finned tubular ceramic membrane were compared. Subsequently, the fin structure of FTCM was optimized based on the study of effects of fin height and pitch of FTCMs on membrane condensation. Finally, effects of operation parameters (flue gas temperature, dry gas flowrate, cooling water temperature as well as cooling water flowrate) on water and waste heat recovery performance were investigated. Our findings are significant in improving condensation performance of TMCs and sustainable energy-water-environment nexus in thermal power plants.

2. Materials and methods

2.1. Original ceramic membranes

Commercial symmetric tubular ceramic membranes with an average pore size of 200 nm were purchased from Nanjing Hongyi Ceramic Nanofiltration Membranes Co., Ltd., China. The porosity was determined using Archimedes' method. The pore size distribution was determined using a microfiltration membrane porosimeter (PSDA-20, GaoQ, China). Fig. 2 shows the pore size distribution of the ceramic membrane. The parameters of original ceramic membranes are listed in Table 2.

2.2. PTCM, FTCM, and WTCM

This study investigates the wet flue gas condensation on one PTCM, five FTCMs, and two WTCMs (Fig. 3). Table 3 shows the geometrical parameters of these tubular ceramic membranes. Fig. 4 is the schematic

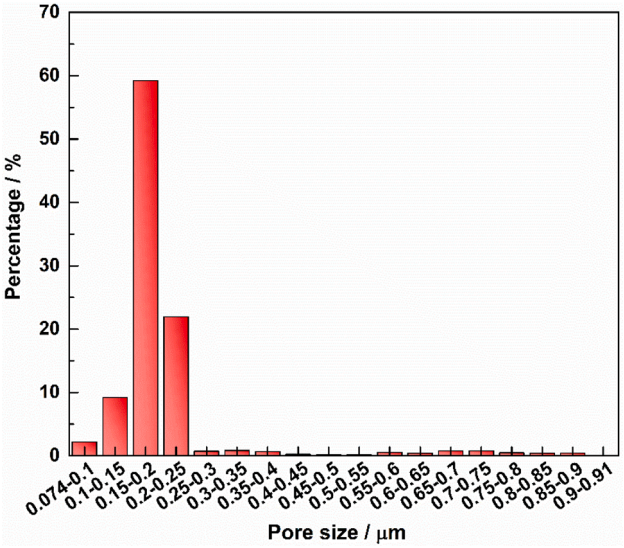

Fig. 2. Pore size distribution of the original ceramic membrane.

Table 2
Parameters of Original Ceramic Membranes.

Parameter	Value
Material	Alumina
Average pore size (nm)	200
Porosity	33%
Length (mm)	500
Inner diameter (mm)	7.2
Outer diameter (mm)	13
Wall thickness (mm)	2.9

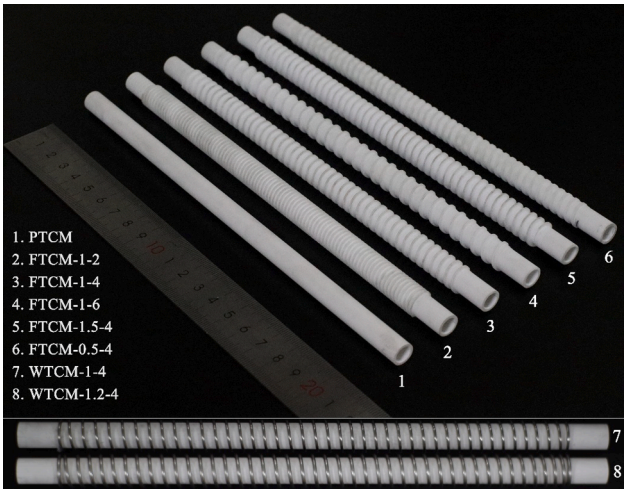

Fig. 3. Images of surface-enhanced ceramic membranes.

Table 3
Geometrical Parameters of Surface-enhanced Ceramic Membranes.

Test specimens	Inner diameter (d_i, mm)	Outer diameter (d_o, mm)	Fin height / Wire diameter (h_f / d_w, mm)	Fin pitch / Wire pitch (p_f / p_w, mm)	Tube type
PTCM	7.2	9.2	/	/	Plain tube
FTCM-0.5–4	7.2	9.2	0.5	4	Fin tube
FTCM-1–2	7.2	9.2	1	2	
FTCM-1–4	7.2	9.2	1	4	
FTCM-1–6	7.2	9.2	1	6	
FTCM-1.5–4	7.2	9.2	1.5	4	
WTCM-1–4	7.2	9.2	1	4	Wire-wrapped tube
WTCM-1.2–4	7.2	9.2	1.2	4	

of structural parameters of FTCMs and WTCMs. The PTCM and FTCMs are obtained by grinding original symmetric tubular ceramic membranes with modified CNC lathe and special cutting tools (Yixing Heheng Precision Ceramics Co., Ltd., China). FTCMs are prepared directly by isostatic pressing in our following study to compare its preparation cost with machining. The WTCMs are obtained by winding different steel wires on the surface of PTCM. The PTCM (without any external structure) is used for comparison. Pure water permeability of the PTCM was measured using a cross-flow filtration system, which is 830 $L{\cdot}m^{-2}{\cdot}h^{-1}{\cdot}bar^{-1}$. For convenient comparison, all ceramic membranes used in this study have the same length (210 mm) and plain inner surface. The values of outer diameter of FTCMs and WTCMs in Table 3 are based on the plain part. In total, the FTCMs have three different fin pitches and fin heights. The fin pitch is defined as the axial center distance of two adjacent fins. The fin profile resembles a trapezoid and fin

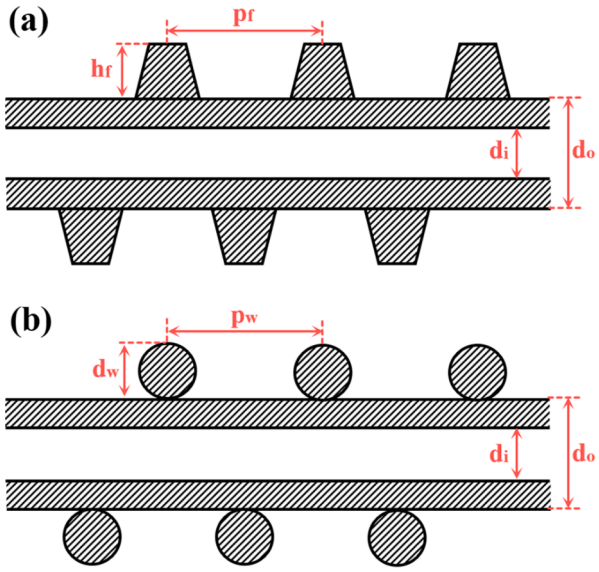

Fig. 4. Schematic of structural parameters of (a) FTCM and (b) WTCM.

thickness at the fin root is about 1.2 mm. The steel wires are 1 mm and 1.2 mm in diameter, respectively. The fin and steel wire segments have the same length of 180 mm. The effective length of ceramic membranes sealed in the module is 170 mm.

2.3. Experimental setup

A bench-scale experimental system was set up to evaluate membrane condensation performance. This system consists of four main parts: membrane module, gas system, cooling water system, and measurement system (Fig. 5). The operation parameters of membrane condensation are summarized in Table 4. The shell-and-tube membrane module was arranged horizontally, and consisted of a stainless-steel shell (inner diameter 14.6 mm) and a tubular ceramic membrane (i.e., PTCM, FTCM, or WTCM). Flue gas flowed at the shell side of the membrane module, whereas cooling water was circulated counter-currently at the tube side.

Wet flue gas was simulated through introducing dry gas into the vapor generator to mix with the vaporized pure water. The dry gas is supplied by air compressor and dehydrated. The dry gas flowrate was measured using the mass flow controller (MQV0050B, Azbil, China). The vapor generator power was adjusted with the aim of controlling the initial temperature of the mixed gas. Subsequently, the gas mixture was introduced into the dehumidification tank and electric heater to achieve the desired humidity. The whole experimental section was well wrapped

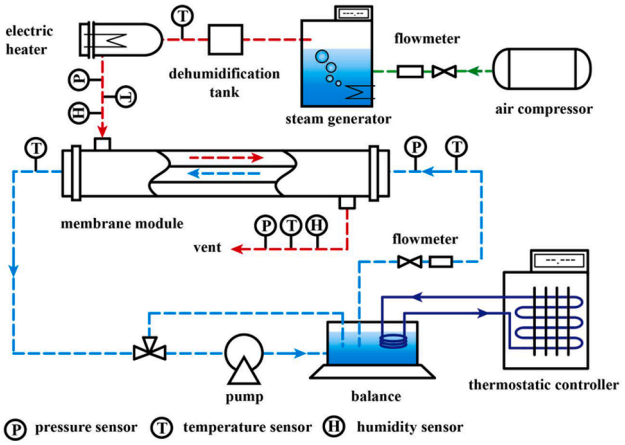

Fig. 5. Schematic of the experimental setup.

Table 4
Operation Parameters of Membrane Condensation.

Operation parameter	Value(s)
Flue gas temperature (°C)	50, 55, 60, 65, 70, 75
Relative humidity	100%
Dry gas flowrate (SLM, 101.325 kPa, 20 °C)	6, 9, 12, 15, 18, 21, 24
Cooling water temperature (°C)	20, 24, 28, 32, 36
Cooling water flowrate (L·min^{-1})	0.2, 0.4, 0.6, 0.8, 1
Transmembrane pressure difference (kPa)	10

Note: SLM represents standard liter per minute.

with thermal insulation materials to curb heat loss to surroundings. The pump at the outlet of membrane module maintained a slight negative pressure (−10 kPa) on water side for the condensate to permeate through the membrane. The liquid flowmeter was utilized to detect cooling water flowrate. A chiller was used to control the cooling water temperature. The weight change of cooling water was monitored with a balance (CP2102, OHAUS, China).

The pressure and temperature transmitters (MIK-P300/MIK-P202, Asmik, China) were installed near the inlet and outlet of flue gas and water to measure the pressure and temperature, respectively. Flue gas relative humidity was measured using humidity sensor (HMT337, Vaisala, Finland). Once the stable values are reached, the data acquisition system records all of the operation parameters (i.e., temperature, humidity, flowrate and pressure) for half an hour at an interval of one minute. There is no bubble at the outlet of cooling water in all tests, suggesting that experimental ceramic membranes possess outstanding selectivity toward the condensable gas. The main test equipment is listed in Table A1 (see Appendix A).

2.4. Flue gas condensation process and HTE

Vapor condensation in the existence of the non-condensable gas, which has relatively low condensing heat transfer coefficient, is quite different from pure vapor condensation.[6] Fig. 6 shows the heat and mass transfer process in wet flue gas condensation using indirect cooling method. When the flue gas flows in the condenser, vapor and non-condensable gases diffuse from the gas bulk to the cold wall. As the local temperature is lower than dew point, the vapor condenses. Afterwards, a condensate film is generated on the hydrophilic wall, and the non-condensable gas boundary layer is formed between the condensate film and gas bulk. In the non-condensable gas boundary layer, convective heat and mass transfer of flue gas occur and sensible heat (Q_s) is released. Vapor condenses and releases latent heat (Q_l) at the gas–liquid interface. The driving forces of the convection mass and heat transfers derive from the differences in the partial pressure and temperature between the interface and gas bulk, correspondingly. Subsequently, the total heat (Q_t) is successively transferred to water side through the condensate film, wall, as well as the water-side boundary layer.[40] Using porous wall instead of dense wall, condensate can permeate to the water side and no condensate accumulation is observed on the membrane surface. That is, condensate film could be eliminated.[17,25] Heat transfer enhancement at the gas side of TMC is primarily aimed at destroying the gas boundary layer. Surface-enhanced tubes and other enhancers can effectively improve the heat transfer by introducing chaotic fluid mixing between the core region and wall, thus promoting turbulence intensity near the tube wall. Besides, periodic vortexes generated by enhancers can immediately destroy the newly formed boundary layer along the flow path.[34]

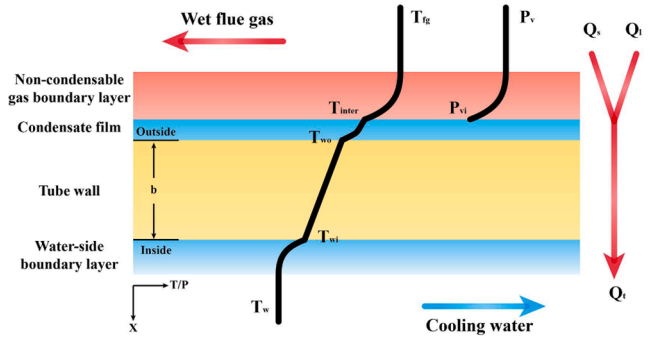

Fig. 6. Schematic of flue gas condensation by indirect cooling.

2.5. Data reduction

2.5.1. Water recovery performance

The water flux (J_w) and water recovery efficiency (γ_w) can be calculated as below:

$$J_w = \frac{\dot{m}_{w,out} - \dot{m}_{w,in}}{A_o} = \frac{\Delta m}{2\pi r_0 L \Delta t} \tag{1}$$

$$\gamma_w = \frac{\dot{m}_{w,out} - \dot{m}_{w,in}}{\dot{m}_{vap,in}} \times 100\% = \frac{\Delta m}{\dot{m}_{dry} x_{in} \Delta t} \times 100\% \tag{2}$$

where $\dot{m}_{w,in}$ and $\dot{m}_{w,out}$ represent the circulating water flowrates at the inlet and outlet of membrane module (kg·h^{-1}), respectively. A_o denotes the effective surface area (m^2) based on the outer radius of plain part (r_o, m), L represents the effective length of the tubular membrane (m), and Δm stands for the circulating water mass change (kg) during a period of time Δt (h). $\dot{m}_{dry}$ and $\dot{m}_{vap,in}$ denote the mass flowrates of dry gas and inlet vapor (kg·h^{-1}), respectively. x represents the mixing ratio (vapor mass/dry gas mass).

The condensing flux (J_g) is calculated by the gas-side parameters:

$$J_g = \frac{\dot{m}_{vap,in} - \dot{m}_{vap,out}}{A_o} = \frac{\dot{m}_{dry}(x_{in} - x_{out})}{2\pi r_o L} \tag{3}$$

2.5.2. Waste heat recovery performance

The heat flux (q_w) and heat recovery efficiency (η_w) are calculated by:

$$q_w = \frac{Q_w}{A_o} = \frac{C_w \dot{m}_{w,in} \Delta T + \dot{m}_t h(T)}{A_o} \tag{4}$$

$$\eta_w = \frac{q_w A_o}{\dot{m}_{dry} h_{in}} \times 100\% \tag{5}$$

where Q_w represents the heat flow (kJ·h^{-1}), C_w denotes the water specific heat capacity (kJ·kg^{-1}·K^{-1}), ΔT represents the circulating water temperature change (K), $h(T)$ stands for the specific enthalpy of water (kJ·kg^{-1}) under a temperature of T, $\dot{m}_t$ denotes the condensate permeation rate (kg·h^{-1}), and h_{in} represents the inlet gas specific enthalpy (kJ·kg^{-1}).

2.5.3. Heat transfer analysis

The total heat transfer coefficient (U_o) can be acquired through:

$$U_o = \frac{Q_w}{A_o \Delta T_m} \tag{6}$$

The logarithmic mean temperature difference (ΔT_m) can be counted utilizing:

$$\Delta T_m = \frac{(T_{g,in} - T_{w,out}) - (T_{g,out} - T_{w,in})}{\ln\left(\frac{T_{g,in} - T_{w,out}}{T_{g,out} - T_{w,in}}\right)} \tag{7}$$

where $T_{g,in}$, $T_{g,out}$, $T_{w,in}$, and $T_{w,out}$ are the temperatures (K) of inlet gas, outlet gas, inlet water, and outlet water, respectively.

The heat transfer coefficients can be counted through employing resistance-in-series model:[31]

$$U_o = \frac{1}{\frac{1}{h_o} + \frac{A_o}{2\pi\lambda_t L} ln\frac{r_o}{r_i} + \frac{A_o}{A_i}\frac{1}{h_i}}, U_o A_o = \frac{1}{\sum R_{th}} \tag{8}$$

where r_i is the inner radius (m), A_i denotes the internal surface area of the tubular membrane (m^2); h_o represents the gas-side heat transfer coefficient, containing condensing and convective heat transfer ($W{\cdot}m^{-2}{\cdot}K^{-1}$); R_{th} is the thermal resistance ($K{\cdot}W^{-1}$); h_i stands for the water-side convective heat transfer coefficient ($W{\cdot}m^{-2}{\cdot}K^{-1}$). λ_t refers to the thermal conductivity of porous membrane impregnated with water ($W{\cdot}m^{-1}{\cdot}K^{-1}$), which is detected via:[17]

$$\lambda_t = (1-\gamma)\lambda_a + \gamma\lambda_w \tag{9}$$

where γ refers to the membrane porosity, λ_w and λ_a represent the thermal conductivities of water and alumina ($W{\cdot}m^{-1}{\cdot}K^{-1}$), respectively.

The thermal resistance of tube wall (R_t) can be expressed as:

$$R_t = \frac{1}{2\pi\lambda_t L} ln\frac{r_o}{r_i} \tag{10}$$

The thermal resistance in circulating water side (R_w) can be determined by:

$$R_w = \frac{1}{h_i A_i} \tag{11}$$

The water flow is in the laminar flow state in this work. By applying Sieder–Tate correlation, the water-side convective heat transfer coefficient can be calculated.[20]

$$h_i = \frac{\lambda_w Nu}{d_i} = 1.86 \times \frac{\lambda_w}{d_i}\left(RePr\frac{d_i}{L}\right)^{\frac{1}{3}}\left(\frac{\mu}{\mu_w}\right)^{0.14} \tag{12}$$

where d_i is the inner diameter (m), *Nu*, *Re* and *Pr* are the Nusselt number, Reynolds number, as well as Prandtl number, and μ denotes the viscosity (Pa·s).

Thus, the gas-side heat transfer coefficient (h_o) along with thermal resistance (R_g) are counted using the following expression:

$$h_o = \frac{1}{R_g A_o}, R_g = \frac{1}{U_o A_o} - R_t - R_w \tag{13}$$

The maximum uncertainties of the water flux (J_w), water recovery efficiency (γ_w), heat flux (q_w), heat recovery efficiency (η_w), pressure drop (dP/dz), and total heat transfer coefficient (U_o) are estimated to be 3.24%, 3.26%, 3.39%, 3.44%, 1.19%, and 3.85%, respectively.

3. Results and discussion

3.1. Condensation experiments of PTCM, FTCM, and WTCM

Condensation experiments were conducted using different surface-enhanced tubular ceramic membranes under consistent operation parameters. The condensing performance of the gas side is evaluated using the gas-side heat transfer coefficient (h_o). h_o is jointly determined by condensing and convection heat transfer. Fig. 7 exhibits the gas-side heat transfer coefficients of different surface-enhanced ceramic membranes at the dry gas flowrate from 6 to 24 SLM. The flowrate of wet flue gas can be represented and calculated by the dry gas volume flowrate in a standard state (20 °C, 101.325 kPa) as the mass of dry gas in the gas path is conserved throughout the experiment. The gas-side heat transfer coefficient rises with the increase of dry gas flowrate owing to stronger shear action and turbulence flow at high gas velocity. Compared with PTCM, all surface-enhanced ceramic membranes exhibit better heat transfer performance. The gas-side heat transfer coefficients of WTCM-1–4, WTCM-1.2–4 and FTCM-1–4 are about 1.3–3.9, 1.3–3.1 and 1.4–2.6 times higher than that of PTCM, respectively. The outcomes of the experiments reveal that the WTCM has the highest heat transfer coefficient. By forming the secondary flows from the membrane surface to the core region, wires promote better fluid mixing near the membrane surface, which enhances heat transfer. It was also observed that the ceramic membrane wrapped with 1 mm wire shows higher heat transfer coefficients than that with 1.2 mm wire at the same pitch. The gap between wires reduces with the increase in wire diameter. This inhibits fluid mixing between the gas bulk and membrane surface. Similar conclusion can be reached in pure vapor condensation process with wire-wrapped tube.[41] Owing to different profiles, the circular cross-section for WTCM and quasi-trapezoidal cross-section for FTCM, fluid mixing and local turbulence vary. The heat transfer performance of FTCM-1–4 is lower than that of WTCM-1–4.

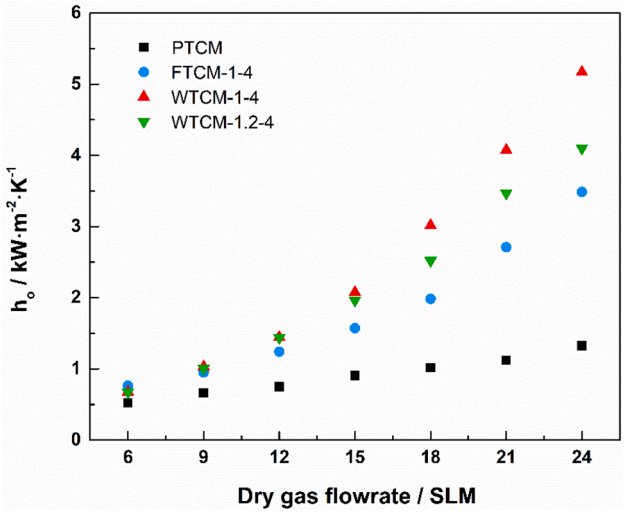

Fig. 7. Gas-side heat transfer coefficients of different surface-enhanced ceramic membranes. Operation parameters: flue gas temperature 60 °C, relative humidity 100%, cooling water temperature 20 °C, cooling water flowrate 0.6 L·min^{-1}.

Fig. 8 shows the pressure drops of different surface-enhanced ceramic membranes at the dry gas flowrate from 6 to 24 SLM. Pressure drops of WTCM and FTCM are higher than that of PTCM. The pressure drops of WTCM-1–4, WTCM-1.2–4 and FTCM-1–4 are about 2.1–3.2, 2.9–4.5 and 1.7–2.7 times higher than that of PTCM, respectively. The WTCM shows the largest loss of pressure as well as the highest gas-side heat transfer coefficient, indicating that the dominant mechanism of enhanced heat transfer is the turbulent effect rather than the surface extension. From Fig. 7 and 8, WTCM-1.2–4 has higher pressure drop but lower heat transfer coefficient than WTCM-1–4. Thus, the structural optimization of surface-enhanced ceramic membranes is

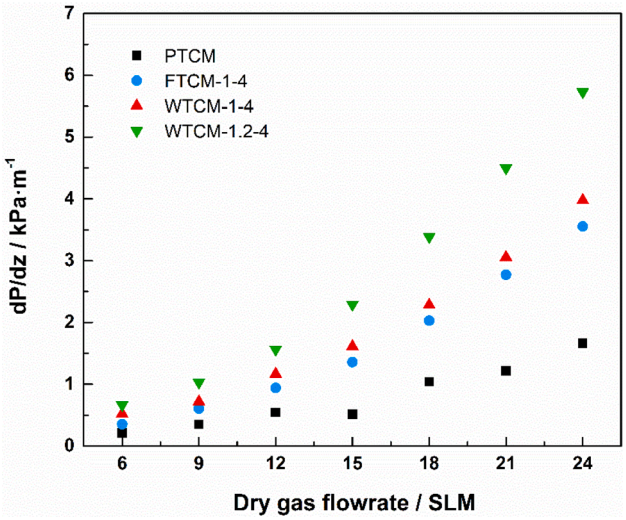

Fig. 8. Pressure drops of different surface-enhanced ceramic membranes. Operation parameters: flue gas temperature 60 °C, relative humidity 100%, cooling water temperature 20 °C, cooling water flowrate 0.6 L·min^{-1}.

also essential.

As illustrated in Fig. 9, for various tubular membranes, the sequence of total heat transfer coefficients (U_o) is as below: WTCM-1–4 > WTCM-1.2–4 > FTCM-1–4 > PTCM. The total heat transfer coefficients of WTCM-1–4 are between 392 and 794 $W{\cdot}m^{-2}{\cdot}K^{-1}$, 37% higher on average than those of PTCM. Fig. 10 shows the thermal resistance distributions of gas side, tube wall and cooling water side for different tubular membranes. The gas-side thermal resistance of PTCM still accounts for 50% of the total resistance at high inlet gas velocity. Clearly, the gas-side convection-condensing heat transfer is one of the main factors influencing the condensing performance of TMC. Although the gas-side thermal resistance of WTCM-1–4 is reduced by 56% compared with that of PTCM, the decline of total thermal resistance is not much (29%) due to the presence of other thermal resistances. Consequently, the improvement of the total heat transfer coefficient is less obvious compared with the gas-side heat transfer coefficient.

Fig. 11 reveals the fluxes of condensed and recovered water of different tubular membranes. It is worth noting that the recovered water of FTCM and PTCM is balanced with the condensed water, respectively, whereas the recovered water of WTCM is slightly less than the condensed water. That is probably because partial condensate on the surface of wires is removed under the action of gravity and gas shear force and could not be recovered in time. Porous fins can enhance heat transfer and increase condensate adsorption area simultaneously. Hence, FTCM is more suitable for water capture from flue gas.

3.2. Effects of fin height and pitch on membrane condensation

Effects of FTCMs with different fin heights (h_f = 0.5, 1 and 1.5 mm) and fin pitches (p_f = 2, 4 and 6 mm) on membrane condensation are presented in this section. Fig. 12 suggests the correlation between the inlet dry gas flowrate and total heat transfer coefficient of PTCM and FTCMs with various fin structures. As seen, FTCM shows higher heat transfer coefficients than PTCM at around 7.4% to 59.3% with different fin structures and operation parameters. It can be found that the effect of fin height on condensation performance is much stronger than that of fin pitch. The total heat transfer coefficient rises with the increase of fin height, as the disturbance of the non-condensable gas boundary layer and turbulence flow can be facilitated through high fins. The heat transfer coefficient of FTCM with h_f = 1.5 mm is higher than that with h_f = 0.5 and 1 mm in a range of 27–38% and 13–20%, respectively. In the case of FTCM with the largest pitch, p_f = 6 mm, compared with PTCM,

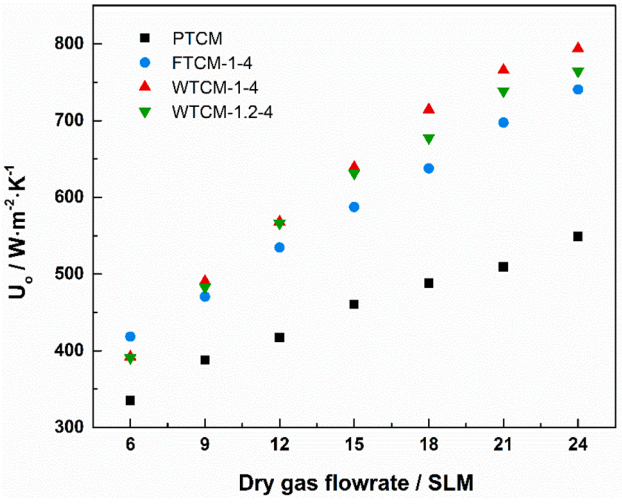

Fig. 9. Total heat transfer coefficients of different surface-enhanced ceramic membranes. Operation parameters: flue gas temperature 60 °C, relative humidity 100%, cooling water temperature 20 °C, cooling water flowrate 0.6 L·min^{-1}.

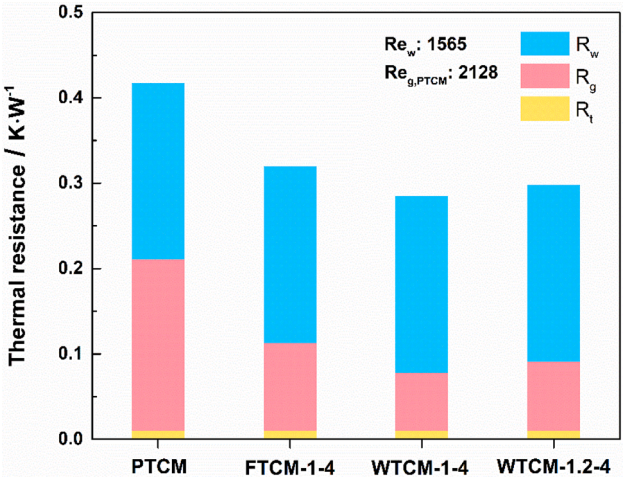

Fig. 10. Thermal resistance distribution of different surface-enhanced ceramic membranes. Operation parameters: flue gas temperature 60 °C, relative humidity 100%, dry gas flowrate 18 SLM, cooling water temperature 20 °C, cooling water flowrate 0.6 L·min^{-1}.

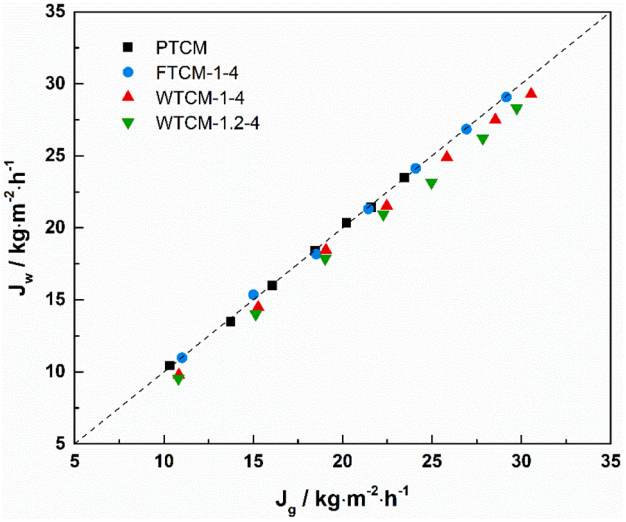

Fig. 11. Comparison of condensed and recovered water. Operation parameters: flue gas temperature 60 °C, relative humidity 100%, cooling water temperature 20 °C, cooling water flowrate 0.6 L·min^{-1}.

the heat transfer coefficient increases by approximately 17–47%. Besides, the heat transfer coefficient of FTCM with p_f = 6 mm is higher than that with p_f = 2 and 4 mm. It is worth noting that the total heat transfer coefficient rises with the increase of fin pitch at high inlet gas flowrate. This may be ascribed to better mixing between the core and tube wall gas due to more efficient turbulence/recirculation flow [34] between the finned surface elements. A gas stagnation region with low gas velocity exists between the fins. As the spacing of fins becomes larger, gas can easily penetrate into the root of fins, improving heat transfer. FTCM with small fin pitch shows better heat transfer performance at low inlet gas flowrate. This means that the mechanism of heat transfer enhancement at low gas velocity is dominated by surface extension at the fin tip rather than turbulence effect. To sum up, large fin height and pitch are obviously helpful to enhance the heat transfer property of FTCM.

Effects of the fin structure of FTCM on pressure drop is shown in Fig. 13. The pressure drop of FTCM gradually rises with the increase of gas flowrate. With the identical test conditions, pressure drops of FTCMs are uniformly higher than that of the PTCM. This may result from the dissipation of dynamic pressure of flue gas caused by turbulence/

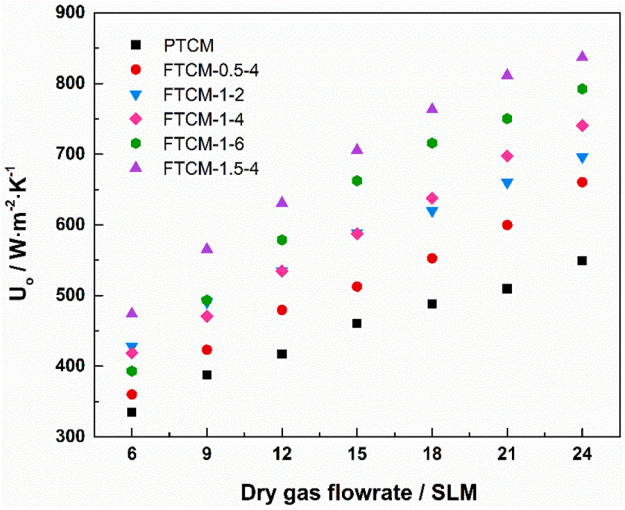

Fig. 12. Effects of fin height and pitch on total heat transfer coefficient of FTCM. Operation parameters: flue gas temperature 60 °C, relative humidity 100%, cooling water temperature 20 °C, cooling water flowrate 0.6 L·min^{-1}.

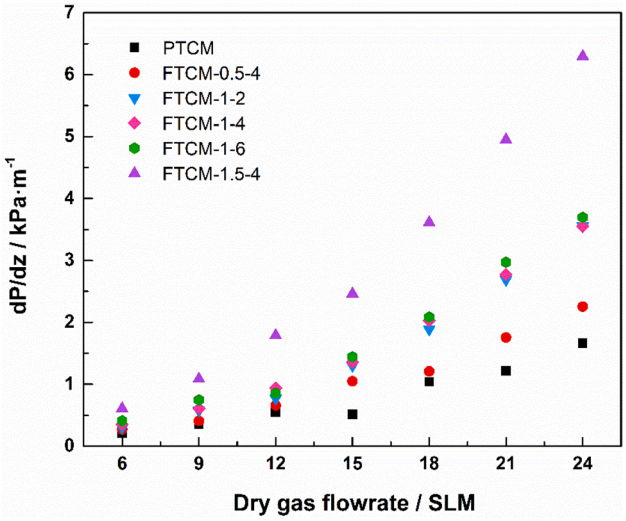

Fig. 13. Effects of fin height and pitch on pressure drop of FTCM. Operation parameters: flue gas temperature 60 °C, relative humidity 100%, cooling water temperature 20 °C, cooling water flowrate 0.6 L·min^{-1}.

recirculation flow and high viscosity losses near the wall.[34] As can be seen in Fig. 13, pressure drop is more sensitive to fin height than to fin pitch. Throughout the experimental results, FTCM with fin height of 1 mm and fin pitch of 6 mm exhibits relatively high heat transfer performance, with relatively low pressure drop. Compared with pure vapor condensation with fin height of 0.45 mm and pitch of 2 mm, fin height and pitch of relatively large size are suitable for membrane condensation process. The enhancement of pure vapor condensation is aimed at reducing the insulating effect of condensate retention in fin channels, [42] whereas thinning the non-condensable gas boundary layer is the key to improve membrane condensation performance.

Fig. 14 illustrates the relationship between dry gas flowrate and water/heat recovery performance of FTCMs. The water/heat recovery performance for different tubular ceramic membranes is in the following sequence: FTCM-1.5–4 > FTCM-1–6 > FTCM-1–4 > FTCM-1–2 > FTCM-0.5–4 > PTCM. Water/heat fluxes drastically increase with the rise of dry gas flowrate. Take FTCM-1–6 for example, as the dry gas flowrate rose from 6 to 24 SLM, the water flux increased from 10.8 to 30.5 kg·m^{-2}·h^{-1}, and the heat flux increased from 30.8 to 85.7 MJ·m^{-2}·h^{-1}. Since latent heat is the major heat source, the variation trend of heat flux is similar to that of water flux. Obviously, the increasing flue gas velocity improves the turbulence of gas side, and the water vapor mass transfer resistance is reduced at the same time. In addition, more water vapor enters TMC under high dry gas flowrate. Thus, a higher condensation rate and improvement in water/heat fluxes are obtained. On the contrary, the water/heat recovery efficiency reduces with the rising dry gas flowrate. As can be seen in Fig. 14b, d, when dry gas flowrate rose from 6 to 24 SLM, the efficiency of water recovery of FTCM-1–6 decreased from 80.8% to 57.6%, and accordingly, the heat recovery efficiency reduced from 76.8 to 53.7%. Gas residence time is a critical factor affecting water/heat recovery efficiency of heat exchangers. With the increase of flue gas flowrate, the residence time of wet flue gas was shortened, causing a mass of unrecovered vapor in the exhaust.[43]

3.3. Effects of operation parameters on membrane condensation using FTCM

The effects of operation parameters including flue gas temperature, cooling water flowrate and cooling water temperature on water/heat recovery performance of FTCM are analyzed (see Text A1 in Appendix A for detail). Increasing the temperature of flue gas effectively improves the water/heat flux. However, the water/heat recovery efficiency tardily improves first and then declines. Water/heat recovery performance slightly improves as the cooling water flow rises. With a rise in the temperature of cooling water, water/heat flux and recovery efficiency significantly reduce. These trends are consistent with previous research using conventional tubular ceramic membranes.[30]

3.4. Comparison of water recovery performance using different membrane materials

Maximum water flux and recovery efficiency can be used to qualitatively compare the water recovery performance of different membrane materials.[44] As summarized in Table 5, porous ceramic membranes exhibit better water recovery performance in contrast to organic membranes. Moreover, FTCM used in this work is more effective in recovering water than conventional configurations of ceramic membranes. Based on this work, it is envisaged that TMC constructed by FTCMs is an efficient water recovery equipment to alleviate water-energy-environment collisions in power plants.

4. Conclusion

In summary, we first report wire-wrapped and helically-finned tubular ceramic membranes for enhancing water and heat recovery performance in wet flue gas condensation. A comparison of water recovery and heat transfer performances of WTCM, FTCM and conventional PTCM was performed. Effects of fin pitch, fin height, dry gas flowrate, flue gas temperature, cooling water flowrate as well as cooling water temperature on membrane condensation were also examined in detail. The major conclusions are summarized as follows.

1. In comparison with conventional PTCM, WTCM and FTCM exhibit superior flue gas condensation performance. The gas-side heat transfer coefficient ratio of surface-enhanced membrane to plain membrane is 1.3–3.9 for WTCM-1–4 and 1.4–2.6 for FTCM-1–4, respectively. The pressure drop ratio of surface-enhanced membrane to plain membrane is 2.1–3.2 for WTCM-1–4 and 1.7–2.7 for FTCM-1–4, respectively. Larger wire diameter of WTCM results in greater pressure drop but poorer condensation performance. The WTCM shows the largest pressure drop and the highest gas-side heat transfer coefficient. FTCM has better condensate capture performance than WTCM.
2. The water/heat recovery performance for FTCM with various fin structures is in the following sequence: FTCM-1.5–4 > FTCM-1–6 >

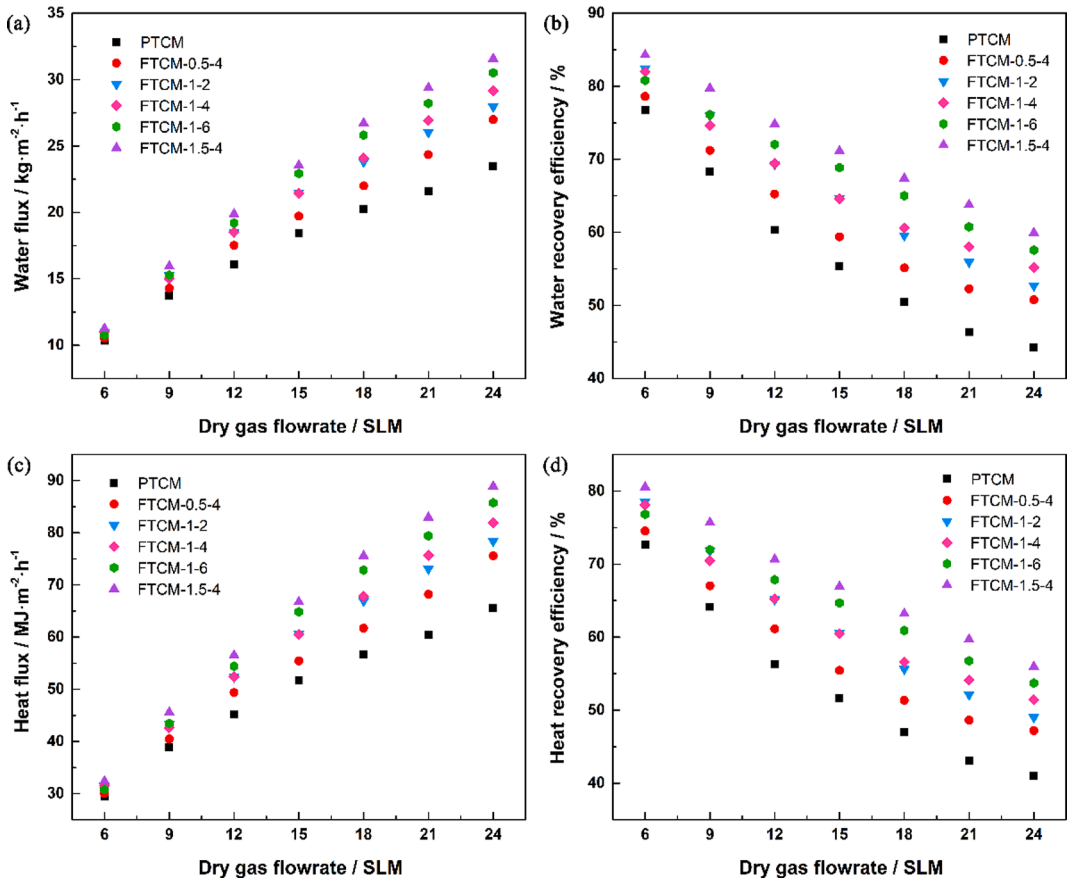

Fig. 14. Effects of dry gas flowrate on water/heat recovery performance of FTCM. Operation parameters: flue gas temperature 60 °C, relative humidity 100%, cooling water temperature 20 °C, cooling water flowrate 0.6 L·min^{-1}.

Table 5
Performances of Different Membrane Materials for Flue Gas Dehumidification.

Materials	Configurations	Characteristics	Maximum water flux (kg·m^{-2}·h^{-1})	Maximum water recovery efficiency	Reference
SPEEK/PES	Composite hollow fiber	Dense/ hydrophilic	1	Not given	Ref.[12]
Hyflon AD40L/PVDF	Composite hollow fiber	Porous/ hydrophobic	0.35	18.85%	Ref.[15]
Ceramic	19-channel tubular	Porous/ hydrophilic	4.2	66%	Ref.[22]
Ceramic	Tubular	Porous/ hydrophilic	21.7	60%	Ref.[28]
Ceramic	Finned tubular	Porous/ hydrophilic	47.8	84.3%	This work

FTCM-1–4 > FTCM-1–2 > FTCM-0.5–4 > PTCM. Improved condensing heat transfer performances are observed on FTCMs provided with large fin height and pitch. Heat transfer coefficient and pressure drop is more sensitive to fin height than to fin pitch.

3. In this work, water flux of 10.3–47.8 kg·m^{-2}·h^{-1} and heat flux of 30.4–130.7 MJ·m^{-2}·h^{-1} were achieved using FTCM.
4. FTCM is more effective in recovering water from flue gas compared to dense polymer membrane, porous hydrophobic organic membrane, and conventional porous ceramic membrane.

The surface-enhanced tubular ceramic membrane is a promising candidate in enhancing water and heat recovery from wet flue gas. Further design of enhanced surface with novel structures is necessary to suit the requirements for better TMC performance. In addition, one-step molding of surface-enhanced ceramic membranes by isostatic pressing may facilitate large-scale applications.

CRediT authorship contribution statement

Chao Ji: Conceptualization, Methodology, Formal analysis, Investigation, Visualization, Data curation, Validation, Writing – original draft. **Wei Liu:** Methodology, Investigation, Visualization. **Hong Qi:** Resources, Validation, Writing – review & editing, Funding acquisition, Project administration, Supervision.

Declaration of Competing Interest

The authors declare that they have no known competing financial interests or personal relationships that could have appeared to influence the work reported in this paper.

Acknowledgements

This work is supported by the National Natural Science Foundation of China (21490581), China Petroleum & Chemical Corporation (317008-6).

Appendix A. Supplementary material

Supplementary data to this article can be found online at https://doi.

org/10.1016/j.seppur.2022.120727.

References

[1] J.F. Kim, E. Drioli, Transport membrane condenser heat exchangers to break the water-energy nexus-a critical review, Membranes 11 (1) (2021) 12, https://doi.org/10.3390/membranes11010012.

[2] D. Gao, Z. Li, H. Zhang, H. Chen, C. Cheng, K. Liang, Moisture and latent heat recovery from flue gas by nonporous organic membranes, J. Clean. Prod. 225 (2019) 1065–1078.

[3] J. Zhang, Z. Li, H. Zhang, H. Chen, D. Gao, Numerical study on recovering moisture and heat from flue gas by means of a macroporous ceramic membrane module, Energy 207 (2020) 118230, https://doi.org/10.1016/j.energy.2020.118230.

[4] C. Cheng, Z. Heng, H. Chen, Experimental study on water recovery from flue gas using macroporous ceramic membrane, Materials 13 (2020) 804.

[5] Z. Wang, X. Zhang, Z. Li, Evaluation of a flue gas driven open absorption system for heat and water recovery from fossil fuel boilers, Energ. Convers. Manage. 128 (2016) 57–65.

[6] W. Zhong, W. Ji, X. Cao, Y. Yuan, Flue gas water recovery by indirect cooling technology for large-scale applications: a review, J. Therm. Sci. 29 (2020) 1223–1241.

[7] A. Brunetti, F. Macedonio, G. Barbieri, E. Drioli, Membrane condenser as emerging technology for water recovery and gas pre-treatment: current status and perspectives, BMC Chemical Engineering 1 (2019) 19.

[8] Z. Wang, X. Zhang, J. Han, Z. Li, Waste heat and water recovery from natural gas boilers: Parametric analysis and optimization of a flue-gas-driven open absorption system, Energ. Convers. Manage. 154 (2017) 526–537.

[9] Q. Chen, K. Finney, H. Li, X. Zhang, J. Zhou, V. Sharifi, J. Swithenbank, Condensing boiler applications in the process industry, Appl. Energ. 89 (2012) 30–36.

[10] Y. Xiong, H. Tan, Y. Wang, W. Xu, H. Mikulcic, N. Duic, Pilot-scale study on water and latent heat recovery from flue gas using fluorine plastic heat exchangers, J. Clean. Prod. 161 (2017) 1416–1422.

[11] D. Gao, Z. Li, H. Zhang, J. Zhang, H. Chen, H. Fu, Moisture recovery from gas-fired boiler exhaust using membrane module array, J. Clean. Prod. 231 (2019) 1110–1121.

[12] H. Sijbesma, K. Nymeijer, R. van Marwijk, R. Heijboer, J. Potreck, M. Wessling, Flue gas dehydration using polymer membranes, J. Membrane Sci. 313 (2008) 263–276.

[13] F. Macedonio, A. Brunetti, G. Barbieri, E. Drioli, Membrane Condenser as a New Technology for Water Recovery from Humidified "Waste" Gaseous Streams, Ind. Eng. Chem. Res. 52 (2013) 1160–1167.

[14] F. Macedonio, A. Brunetti, G. Barbieri, E. Drioli, Membrane condenser configurations for water recovery from waste gases, Sep. Purif. Technol. 181 (2017) 60–68.

[15] J. Cao, J. Pan, Z. Cui, Z. Wang, X. Wang, E. Drioli, Improving efficiency of PVDF membranes for recovering water from humidified gas streams through membrane condenser, Chem. Eng. Sci. 210 (2019), 115234.

[16] D. Wang, A. Bao, W. Kunc, W. Liss, Coal power plant flue gas waste heat and water recovery, Appl. Energ. 91 (2012) 341–348.

[17] A. Bao, D. Wang, C. Lin, Nanoporous membrane tube condensing heat transfer enhancement study, Int. J. Heat Mass Tran. 84 (2015) 456–462.

[18] S. Zhao, S. Yan, D.K. Wang, Y. Wei, H. Qi, T. Wu, P.H.M. Feron, Simultaneous heat and water recovery from flue gas by membrane condensation: Experimental investigation, Appl. Therm. Eng. 113 (2017) 843–850.

[19] H. Chen, Y. Zhou, S. Cao, X. Li, X. Su, L. An, D. Gao, Heat exchange and water recovery experiments of flue gas with using nanoporous ceramic membranes, Appl. Therm. Eng. 110 (2017) 686–694.

[20] Z. Li, H. Zhang, H. Chen, J. Zhang, C. Cheng, Experimental research on the heat transfer and water recovery performance of transport membrane condenser, Appl. Therm. Eng. 160 (2019), 114060.

[21] H. Chen, Y. Zhou, X. Su, S. Cao, Y. Liu, D. Gao, L. An, Experimental study of water recovery from flue gas using hollow micro-nano porous ceramic composite membranes, J. Ind. Eng. Chem. 57 (2018) 349–355.

[22] M. Yue, S. Zhao, P.H.M. Feron, H. Qi, Multichannel Tubular Ceramic Membrane for Water and Heat Recovery from Waste Gas Streams, Ind. Eng. Chem. Res. 55 (2016) 2615–2622.

[23] Y. Cao, L. Wang, C. Ji, Y. Huang, Z. Xue, J. Lu, H. Qi, Pilot-scale application on dissipation of smoke plume from flue gas using ceramic membrane condensers, CIESC Journal 70 (2019) 2192–2201.

[24] C. Cheng, D. Liang, Y. Zhang, H. Zhang, H. Chen, D. Gao, Pilot-scale study on flue gas moisture recovery in a coal-fired power plant, Sep. Purif. Technol. 254 (2021), 117254.

[25] H.W. Hu, G.H. Tang, D. Niu, Wettability modified nanoporous ceramic membrane for simultaneous residual heat and condensate recovery, Sci. Rep. 6 (2016) 27274.

[26] L. Xiao, M. Yang, S. Zhao, W. Yuan, S. Huang, Entropy generation analysis of heat and water recovery from flue gas by transport membrane condenser, Energy 174 (2019) 835–847.

[27] S. Soleimanikutanaei, C. Lin, D. Wang, Numerical modeling and analysis of Transport Membrane Condensers for waste heat and water recovery from flue gas, Int. J. Therm. Sci. 136 (2019) 96–106.

[28] T. Wang, M. Yue, H. Qi, P.H.M. Feron, S. Zhao, Transport membrane condenser for water and heat recovery from gaseous streams: Performance evaluation, J. Membrane Sci. 484 (2015) 10–17.

[29] Q. Meng, Y. Cao, Y. Huang, L. Wang, L. Li, S. Niu, H. Qi, Effects of process parameters on water and waste heat recovery from flue gas using ceramic ultrafiltration membranes, CIESC Journal 69 (2018) 2519–2525.

[30] C. Ji, L. Li, H. Qi, Improving heat transfer and water recovery performance in high-moisture flue gas condensation using silicon carbide membranes, Int. J. Energ. Res. 45 (2021) 10974–10988.

[31] Q. Cao, Q. Meng, C. Ji, S. Niu, L. Li, H. Qi, Effect of pore size of outer-coated ceramic membranes on water and heat recovery performance in flue gas, Membrane Science and Technology (Chinese) 41 (4) (2021) 102–109.

[32] Z. Li, H. Zhang, H. Chen, Application of transport membrane condenser for recovering water in a coal-fired power plant: A pilot study, J. Clean. Prod. 261 (2020), 121229.

[33] J.F. Kim, A. Park, S. Kim, P. Lee, Y. Cho, H. Park, S. Nam, Y. Park, Harnessing clean water from power plant emissions using membrane condenser technology, Acs Sustain. Chem. Eng. 6 (2018) 6425–6433.

[34] S. Pethkool, S. Eiamsa-ard, S. Kwankaomeng, P. Promvonge, Turbulent heat transfer enhancement in a heat exchanger using helically corrugated tube, Int. Commun. Heat Mass 38 (2011) 340–347.

[35] M. Dilaver, S.M. Hocaoglu, G. Soydemir, M. Dursun, B. Keskinler, I. Koyuncu, M. Agtas, Hot wastewater recovery by using ceramic membrane ultrafiltration and its reusability in textile industry, J. Clean. Prod. 171 (2018) 220–233.

[36] L. Xiao, M. Yang, W. Yuan, S. Huang, Macroporous ceramic membrane condenser for water and heat recovery from flue gas, Appl. Therm. Eng. 186 (2021), 116512.

[37] I.Z. Famileh, J. Esfahani, A., Experimental investigation of wet flue gas condensation using twisted tape insert, Int. J. Heat Mass Tran. 108 (2017) 1466–1480.

[38] Z.-C. Sun, W. Li, X. Ma, Z. Ayub, Y. He, Flow boiling in horizontal annuli outside horizontal smooth, herringbone and three-dimensional enhanced tubes, Int. J. Heat Mass Tran. 143 (2019) 118554, https://doi.org/10.1016/j.ijheatmasstransfer.2019.118554.

[39] H.M. Ali, M.Z. Qasim, M. Ali, Free convection condensation heat transfer of steam on horizontal square wire wrapped tubes, Int. J. Heat Mass Tran. 98 (2016) 350–358.

[40] D.F. Che, Y.D. Da, Z.N. Zhuang, Heat and mass transfer characteristics of simulated high moisture flue gases, Heat Mass Transfer 41 (2005) 250–256.

[41] H.M. Ali, M.Z. Qasim, Free convection condensation of steam on horizontal wire wrapped tubes: Effect of wire thermal conductivity, pitch and diameter, Appl. Therm. Eng. 90 (2015) 207–214.

[42] A.R. Al-Badri, A. Baer, A. Gotterbarm, M.H. Rausch, A.P. Froeba, The influence of fin structure and fin density on the condensation heat transfer of R134a on single finned tubes and in tube bundles, Int. J. Heat Mass Tran. 100 (2016) 582–589.

[43] S. Yan, Q. Cui, T. Tu, L. Xu, Q. He, P.H.M. Feron, S. Zhao, Membrane heat exchanger for novel heat recovery in carbon capture, J. Membrane Sci. 577 (2019) 60–68.

[44] T. Tu, S. Liu, Q. Cui, L. Xu, L. Ji, S. Yan, Techno-economic assessment of waste heat recovery enhancement using multi-channel ceramic membrane in carbon capture process, Chem. Eng. J. 400 (2020), 125677.